Wetting of potassium surfaces by superfluid ^{4}He: A study using variational properties of the chemical potential

Leszek Szybisz*
Laboratorio TANDAR, Departamento de Física, Comisión Nacional de Energía Atómica, Avenida del Libertador 8250, RA-1429 Buenos Aires, Argentina
and Departamento de Física, Facultad de Ciencias Exactas y Naturales, Universidad de Buenos Aires, Ciudad Universitaria, RA-1428 Buenos Aires, Argentina
(Received 4 January 2000)

The wetting of planar surfaces of K by superfluid ^{4}He films at $T=0$ K is theoretically studied. In order to examine the consistency of numerical results, new variational properties of the chemical potential μ are derived. Two substrate-adsorbate interactions are analyzed: (a) the standard ''3-9'' one and (b) the more elaborated potential recently proposed by Chizmeshya, Cole, and Zaremba (CCZ). New results calculated within the framework of two different nonlocal density functionals (namely, those known as the Orsay-Paris and Orsay-Trento formalisms) are reported. It is demonstrated that the numerical solutions obtained from the theoretical equations verify with high accuracy the derived variational conditions. The main output of this investigation is the finding that, for both analyzed adsorption potentials, thick enough helium films exhibit a positive square of the third-sound velocity. The wetting of a potassium substrate by superfluid ^{4}He at $T=0$ K suggested by experimental data is guaranteed in the case of the recent CCZ potential.

I. INTRODUCTION

The experiment and theory of interfaces and surfaces have been continuously developed during the past decade. The reader may follow the recent progress in Refs. 1–3. A glance at the list of investigated problems indicates that wetting of planar solid substrates by superfluid helium is one of the most studied issues. The interest in this field has been considerably stimulated due to the fact that the analysis of properties of helium films adsorbed on weakly attractive heavy-alkali metals has led to the nonwetting phenomenon.

In 1991 Cheng *et al.*[4] predicted that ^{4}He should not wet planar surfaces of Cs, Rb, and K at $T=0$ K. This fascinating behavior was argued on the basis of results obtained by using a nonlocal density functional (NLDF) theory. In this theoretical framework, the ground-state energy $E_{\rm gs}$ of an inhomogeneous liquid of ^{4}He confined by an external potential due to a substrate, $U_{\rm sub}(\mathbf{r})$, may be written as[5]

$$E_{\rm gs}=-\frac{\hbar^2}{2m}\int d\mathbf{r}\sqrt{\rho(\mathbf{r})}\nabla^2\sqrt{\rho(\mathbf{r})} + \int\int d\mathbf{r}\,d\mathbf{r}'\rho(\mathbf{r})\rho(\mathbf{r}')E_c(\mathbf{r},\mathbf{r}')+\int d\mathbf{r}\,\rho(\mathbf{r})U_{\rm sub}(\mathbf{r}), \tag{1.1}$$

where $\rho(\mathbf{r})$ is the one-body density. The first term on the right-hand side is the quantum kinetic energy of the helium atoms of mass m. The second term represents the interaction between the particles of the liquid, so that the quantity $E_c(\mathbf{r},\mathbf{r}')$ is the correlation energy density depending on the approach adopted for the theoretical description.[5] We shall come back to this point later on. Finally, the last term is the interaction of helium with the external field. The spatial particle distribution $\rho(\mathbf{r})$ is determined by solving an Euler-Lagrange (EL) equation, which is derived by applying a variational procedure with the constraint of a fixed particle number N, i.e.,

$$\frac{\delta[E_{\rm gs}-\mu N]}{\delta\sqrt{\rho(\mathbf{r})}}=0. \tag{1.2}$$

Here μ is the chemical potential and N is defined as

$$N=\int d\mathbf{r}\,\rho(\mathbf{r}). \tag{1.3}$$

The variation of Eq. (1.2) leads to a Hartree-like equation for the square root of the one-body density

$$\left[-\frac{\hbar^2}{2m}\nabla^2+V_H(\mathbf{r})+U_{\rm sub}(\mathbf{r})\right]\sqrt{\rho(\mathbf{r})}=\mu\sqrt{\rho(\mathbf{r})}, \tag{1.4}$$

which also determines μ. Here $V_H(\mathbf{r})$ is a Hartree mean-field potential given by the first functional derivative of the total correlation energy $E_c[\rho]$,

$$V_H(\mathbf{r})=\frac{\delta E_c[\rho]}{\delta\rho(\mathbf{r})}=\frac{\delta}{\delta\rho(\mathbf{r})}\int\int d\mathbf{r}'d\mathbf{r}''\rho(\mathbf{r}')\rho(\mathbf{r}'')E_c(\mathbf{r}',\mathbf{r}''). \tag{1.5}$$

In the case of a planar geometry, the system is translationally invariant in the x-y plane and symmetry is broken in the z direction giving rise to a density profile $\rho(z)$. This scenario may be caused by the action of an external potential of the form $U_{\rm sub}(\mathbf{r})=U_{\rm sub}(z)$.

The theoretical results of Ref. 4 were obtained by using the Orsay-Paris NLDF (OP-NLDF) formulation of Dupont-Roc *et al.*[6] and by assuming that the interaction between helium atoms and the surfaces is described by a simple two-parameter ''3-9'' substrate-adsorbate potential of the form

$$U_{\rm sub}(z)=U_{3\text{-}9}(z)=\left(\frac{4C_3^3}{27D^2}\right)\frac{1}{z^9}-\frac{C_3}{z^3}. \qquad (1.6)$$

Here D is the well depth and C_3 the van der Waals coefficient. Widely used values of these parameters have been derived by Zaremba and Kohn[7] and are listed in Table I of the first cite of Ref. 4.

After the prediction of Cheng *et al.*,[4] a large amount of experimental work in the field was started. An instructive review of the experiments performed in the early 1990s was written by Hallock.[8] In summary, the available information indicates that ^{4}He does not wet Cs at $T=0$ K, but it wets this substrate at temperatures larger than the wetting temperature $T_w \simeq 2$ K.[9–13] In the case of ^{4}He on Rb, the situation is not so clear. The experimental evidence suggests that T_w would be about 0.3 K or perhaps zero.[14–19]

Lighter alkali metals have received less experimental attention.[9,18,20] After taking into account that (i) the adsorption potential deepens as the alkali metal becomes lighter, and (ii) the wetting temperature for ^{4}He on Rb is, if different from zero, much smaller than that found for Cs, it becomes plausible to expect that K, Na, and Li would be wetted by ^{4}He at $T=0$ K. As a matter of fact, recent measurements reported in Ref. 18 show that helium wets potassium and sodium at $T=0$ K. In this context, although there are no experimental data in the case of the Li substrate, it should be mentioned that quite recent path integral Monte Carlo (PIMC) simulations[21,22] show that helium wets lithium.

Due to its extraordinary characteristic, several features related to the nonwetting to wetting transitions have been extensively studied in recent years, becoming one of the goals of the current investigations in this area. So, the contact angle of ^{4}He droplets on Cs was measured.[23–25] Subsequently, Ancilotto, Sartori, and Toigo[26] have reported a new theoretical investigation of the structure and contact angle of ^{4}He droplets adsorbed on a Cs surface. In this study, the calculations were carried out by utilizing the improved NLDF formulation proposed by the Orsay-Trento collaboration[27,28] (OT-NLDF) and the novel substrate-adsorbate potential evaluated by Chizmeshya, Cole, and Zaremba[29] (CCZ potential)

$$\begin{aligned} U_{\rm sub}(z) &= U_{\rm CCZ}(z) \\ &= V_0(1+\alpha z)\exp(-\alpha z) \\ &\quad - f_2[\beta(z)(z-z_{vdW})]\frac{C_{vdW}}{(z-z_{vdW})^3}, \end{aligned} \qquad (1.7)$$

where

$$f_2(x)=1-\left(1+x+\frac{x^2}{2}\right)\exp(-x), \qquad (1.8)$$

and

$$\beta(z)=\frac{\alpha^2 z}{1+\alpha z}. \qquad (1.9)$$

The parameters of these expressions are quoted in Table 1 of Ref. 29. It should be noticed that, for a given substrate, this potential is more attractive than that of Eq. (1.6) with the parameters of Ref. 7. Turning to Ref. 26, the authors could reproduce satisfactorily well the size of the experimental contact angle.[23–25] On the other hand, a PIMC simulation performed by Boninsegni and Cole[30] yielded a wetting transition at a temperature $T_w \sim 2$ K consistent with the experimental value.[9–13] In this study, the authors adopted the Aziz potential[31] to describe the interaction between helium particles, whereas the interaction between the ^{4}He atoms and the Cs surface was modeled by the ''3-9'' potential of Eq. (1.6). In summary, the information available in the literature concerned the adsorption on Cs depicts a consistent pattern.

Let us now look more carefully at the current knowledge about the adsorption of ^{4}He films on K substrate, which was mentioned in the pioneering work[4] as the last candidate to exhibit nonwetting behavior at zero temperature. According to theoretical results obtained with the ''3-9'' potential in Refs. 4 (cf. Table I in the first cite) and 27 (see comments to Fig. 9 therein), the superfluid ^{4}He should not wet flat surfaces of K. To the contrary, more recent estimations performed in Ref. 29 by using the more elaborated CCZ potential indicate that ^{4}He should wet substrates of K at $T=0$ K. The latter prediction is supported by the already mentioned experimental data.[18] So, it remains to establish precisely the origin of the discrepancy between theoretical conclusions drawn in Refs. 4 and 27 and that obtained in Ref. 29. Therefore, we have undertaken a revised study of this problem by performing new variational calculations.

In solving the optimization problem (1.4), the least stable quantity is the chemical potential μ, which therefore exhibits the largest numerical uncertainty. Consequently, it becomes useful to study properties of μ to gain insights as well as to obtain relations that might be utilized to control the consistency of the solutions. Motivated by this fact, in the present work we explore the behavior of the variation of μ when Eq. (1.4) is solved for different values of N. The derived relations are applied to control the consistency of numerical solutions for films of liquid ^{4}He adsorbed on substrates of K. On the basis of these results, we are able to reach a conclusion about wetting.

The structure of this paper is the following. Variational properties of μ are derived in Sec. II. The relevant tools for treating the planar geometry are provided in Sec. III. Section IV is devoted to analyzing the overall consistency of numerical results for liquid ^{4}He adsorbed on K surfaces at zero absolute temperature and to discussing the stability of these systems. Finally, the concluding remarks are given in Sec. V.

II. THE BEHAVIOR OF μ WHEN THE PARTICLE NUMBER IS CHANGED

In the first part of this section, we shall study variational properties of μ for finite changes of N. Subsequently, the limit for infinitesimal variations is analyzed.

A. Variation of μ for finite changes of N

Let us consider solutions of Eq. (1.4) corresponding to two different particle numbers denoted as N_i and $N_f=N_i+\delta N$. At this stage the size of δN remains arbitrary, that is, we are not requiring small changes of N. For N_i, one gets μ_i and $\sqrt{\rho_i(\mathbf{r})}$ satisfying

$$\left[-\frac{\hbar^2}{2m}\nabla^2+V_H^i(\mathbf{r})+U_{\rm sub}(\mathbf{r})\right]\sqrt{\rho_i(\mathbf{r})}=\mu_i\sqrt{\rho_i(\mathbf{r})}, \tag{2.1}$$

while for N_f one obtains μ_f and $\sqrt{\rho_f(\mathbf{r})}$ obeying

$$\left[-\frac{\hbar^2}{2m}\nabla^2+V_H^f(\mathbf{r})+U_{\rm sub}(\mathbf{r})\right]\sqrt{\rho_f(\mathbf{r})}=\mu_f\sqrt{\rho_f(\mathbf{r})}. \tag{2.2}$$

Note that the Hartree mean-field potential present in both these equations is different, the relation may be expressed as $V_H^f(\mathbf{r})=V_H^i(\mathbf{r})+\delta V_H(\mathbf{r})$. Accordingly, the remaining final quantities may also be written as a sum of the initial ones and their variations, i.e., $\mu_f=\mu_i+\delta\mu$ and $\sqrt{\rho_f(\mathbf{r})}=\sqrt{\rho_i(\mathbf{r})}+\delta\sqrt{\rho(\mathbf{r})}$. To simplify the notation, in what follows, we shall drop the index i when referring to $\rho_i(\mathbf{r})$. Upon multiplying both above written equations from the left by the square root of the corresponding one-body density and integrating over $d\mathbf{r}$ one arrives at

$$\int d\mathbf{r}\sqrt{\rho(\mathbf{r})}\left[-\frac{\hbar^2}{2m}\nabla^2+V_H^i(\mathbf{r})+U_{\rm sub}(\mathbf{r})\right]\sqrt{\rho(\mathbf{r})} =\mu_i\int d\mathbf{r}\,\rho(\mathbf{r})=\mu_i N_i, \tag{2.3}$$

and

$$\int d\mathbf{r}[\sqrt{\rho(\mathbf{r})}+\delta\sqrt{\rho(\mathbf{r})}]\left[-\frac{\hbar^2}{2m}\nabla^2+V_H^f(\mathbf{r})+U_{\rm sub}(\mathbf{r})\right] \times[\sqrt{\rho(\mathbf{r})}+\delta\sqrt{\rho(\mathbf{r})}] =\mu_f\int d\mathbf{r}[\sqrt{\rho(\mathbf{r})}+\delta\sqrt{\rho(\mathbf{r})}]^2 =\mu_f N_f. \tag{2.4}$$

Of course, the right-hand side of the latter equation may also be written in terms of the initial quantities and their variations

$$\mu_f N_f=(\mu_i+\delta\mu)(N_i+\delta N)=\mu_i N_i+\mu_i\delta N+\delta\mu(N_i+\delta N). \tag{2.5}$$

Before proceeding further with the analysis of Eq. (2.4), we shall express δN in terms of the initial one-body density and its variation. Starting from the definition of N_f, we obtain

$$N_f=N_i+\delta N=\int d\mathbf{r}[\sqrt{\rho(\mathbf{r})}+\delta\sqrt{\rho(\mathbf{r})}]^2 =\int d\mathbf{r}\,\rho(\mathbf{r})+\int d\mathbf{r}[2\sqrt{\rho(\mathbf{r})}+\delta\sqrt{\rho(\mathbf{r})}]\delta\sqrt{\rho(\mathbf{r})}, \tag{2.6}$$

from where arises

$$\delta N=\int d\mathbf{r}[2\sqrt{\rho(\mathbf{r})}+\delta\sqrt{\rho(\mathbf{r})}]\delta\sqrt{\rho(\mathbf{r})}. \tag{2.7}$$

Perhaps, it is instructive to notice that an alternative way for getting δN consists of evaluating directly the total variation of the particle number

$$\delta N=\delta\int d\mathbf{r}\,\rho(\mathbf{r})=\int d\mathbf{r}\delta\rho(\mathbf{r}) =\int d\mathbf{r}[2\sqrt{\rho(\mathbf{r})}+\delta\sqrt{\rho(\mathbf{r})}]\delta\sqrt{\rho(\mathbf{r})}, \tag{2.8}$$

where use was made of the relation

$$\delta\rho(\mathbf{r})=2\sqrt{\rho(\mathbf{r})}\delta\sqrt{\rho(\mathbf{r})}+[\delta\sqrt{\rho(\mathbf{r})}]^2. \tag{2.9}$$

Let us emphasize that in Eqs. (2.7) and (2.9) the total variation of $\delta\rho(\mathbf{r})$ is kept because at this point, we are calculating the total change of μ when the integrodifferential Eq. (1.4) is solved for two arbitrarily different particle numbers N_i and N_f.

In order to derive a nontrivial equation for $\delta\mu$, we shall split the integral of the left-hand side of Eq. (2.4) into three contributions, performing this procedure in such a way that each term could be related to results obtained in Eqs. (2.1), (2.2), and (2.3)

$$\int d\mathbf{r}[\sqrt{\rho(\mathbf{r})}+\delta\sqrt{\rho(\mathbf{r})}]\left[-\frac{\hbar^2}{2m}\nabla^2+V_H^f(\mathbf{r})+U_{\rm sub}(\mathbf{r})\right][\sqrt{\rho(\mathbf{r})}+\delta\sqrt{\rho(\mathbf{r})}]$$

$$=\int d\mathbf{r}\sqrt{\rho(\mathbf{r})}\left[-\frac{\hbar^2}{2m}\nabla^2+V_H^f(\mathbf{r})+U_{\rm sub}(\mathbf{r})\right]\sqrt{\rho(\mathbf{r})}+\int d\mathbf{r}\sqrt{\rho(\mathbf{r})}\left[-\frac{\hbar^2}{2m}\nabla^2+V_H^f(\mathbf{r})+U_{\rm sub}(\mathbf{r})\right]\delta\sqrt{\rho(\mathbf{r})}$$
$$+\int d\mathbf{r}\delta\sqrt{\rho(\mathbf{r})}\left[-\frac{\hbar^2}{2m}\nabla^2+V_H^f(\mathbf{r})+U_{\rm sub}(\mathbf{r})\right][\sqrt{\rho(\mathbf{r})}+\delta\sqrt{\rho(\mathbf{r})}]$$
$$=\mu_i N_i+\int d\mathbf{r}\sqrt{\rho(\mathbf{r})}\delta V_H(\mathbf{r})\sqrt{\rho(\mathbf{r})}+\int d\mathbf{r}\sqrt{\rho(\mathbf{r})}[\mu_i+\delta V_H(\mathbf{r})]\delta\sqrt{\rho(\mathbf{r})}+\int d\mathbf{r}\delta\sqrt{\rho(\mathbf{r})}[\mu_i+\delta\mu][\sqrt{\rho(\mathbf{r})}+\delta\sqrt{\rho(\mathbf{r})}]$$
$$=\mu_i N_i+\mu_i\delta N+\delta\mu\int d\mathbf{r}[\sqrt{\rho(\mathbf{r})}+\delta\sqrt{\rho(\mathbf{r})}]\delta\sqrt{\rho(\mathbf{r})}+\int d\mathbf{r}\sqrt{\rho(\mathbf{r})}[\sqrt{\rho(\mathbf{r})}+\delta\sqrt{\rho(\mathbf{r})}]\delta V_H(\mathbf{r}). \tag{2.10}$$

Upon inserting the results (2.5) and (2.10) into (2.4) we obtain

$$\int d\mathbf{r}\sqrt{\rho(\mathbf{r})}[\sqrt{\rho(\mathbf{r})}+\delta\sqrt{\rho(\mathbf{r})}]\delta V_H(\mathbf{r}) = \delta\mu\int d\mathbf{r}\sqrt{\rho(\mathbf{r})}[\sqrt{\rho(\mathbf{r})}+\delta\sqrt{\rho(\mathbf{r})}], \quad (2.11)$$

which leads to

$$\delta\mu=\frac{\int d\mathbf{r}\sqrt{\rho(\mathbf{r})}[\sqrt{\rho(\mathbf{r})}+\delta\sqrt{\rho(\mathbf{r})}]\delta V_H(\mathbf{r})}{\int d\mathbf{r}\sqrt{\rho(\mathbf{r})}[\sqrt{\rho(\mathbf{r})}+\delta\sqrt{\rho(\mathbf{r})}]}. \quad (2.12)$$

This is an exact expression for $\delta\mu$ since no contribution has been neglected in the variational calculation. In fact, there is a complete cancellation of terms proportional to $[\delta\sqrt{\rho(\mathbf{r})}]^2$. Furthermore, since no assumption on the size of $\delta\sqrt{\rho(\mathbf{r})}$ was made, this relation is valid for any δN. This form indicates that the variation of the chemical potential is given by a sort of spatially weighted average over local variations of the Hartree mean-field potential

$$\delta\mu=\mu_f-\mu_i=\frac{\int d\mathbf{r}\,\overline{\rho}(\mathbf{r})\,\delta V_H(\mathbf{r})}{\int d\mathbf{r}\,\overline{\rho}(\mathbf{r})} = \frac{\int d\mathbf{r}\,\overline{\rho}(\mathbf{r})[V_H^f(\mathbf{r})-V_H^i(\mathbf{r})]}{\int d\mathbf{r}\,\overline{\rho}(\mathbf{r})}, \quad (2.13)$$

the weight being the geometric average of the involved one-body densities

$$\overline{\rho}(\mathbf{r})=(\rho(\mathbf{r})[\sqrt{\rho(\mathbf{r})}+\delta\sqrt{\rho(\mathbf{r})}]^2)^{1/2}=\sqrt{\rho_i(\mathbf{r})\rho_f(\mathbf{r})}. \quad (2.14)$$

On the basis of this theoretical derivation, we can state that solutions of any system described by Eqs. (1.1) and (1.4) must exhibit variations satisfying the compact relation (2.13). Besides the physical interest of this finding, it is worthy of notice that the numerical verification of this property may provide a good test for the overall self-consistency of evaluated results. The simple structure of Eq. (2.13) makes this proof very easy.

B. The limiting case $\delta N\to 0$

For several reasons it becomes relevant to look at the behavior of $\delta\mu$ for $\delta N\to 0$. In this case, it is of particular interest to evaluate the limit of the ratio $\delta\mu/\delta N$

$$\frac{d\mu}{dN}=\lim_{\delta N\to 0}\left(\frac{\delta\mu}{\delta N}\right)=\frac{1}{N}\int d\mathbf{r}\,\rho(\mathbf{r})\lim_{\delta N\to 0}\left(\frac{\delta V_H(\mathbf{r})}{\delta N}\right), \quad (2.15)$$

then we get

$$N\frac{d\mu}{dN}=\int d\mathbf{r}\,\rho(\mathbf{r})\frac{dV_H(\mathbf{r})}{dN}. \quad (2.16)$$

Quantity $Nd\mu/dN$ plays an important role in the analysis of the stability of liquid ^{4}He films, therefore, we shall return to this point later.

For the sake of completeness, we shall point out that the chemical potential may be expressed in terms of the superposition of the Hartree mean-field and external potentials $V_H(\mathbf{r})+U_{\rm sub}(\mathbf{r})$ and the derivatives of $\sqrt{\rho(\mathbf{r})}$ with respect to N. In order to derive such a formula, one may start differentiating Eq. (2.3) with respect to the particle number

$$\frac{d}{dN}\left(\int d\mathbf{r}\sqrt{\rho(\mathbf{r})}\left[-\frac{\hbar^2}{2m}\nabla^2+V_H(\mathbf{r})+U_{\rm sub}(\mathbf{r})\right]\sqrt{\rho(\mathbf{r})}\right) = \frac{d}{dN}(N\mu). \quad (2.17)$$

This procedure leads to

$$2\int d\mathbf{r}\left(\frac{d\sqrt{\rho(\mathbf{r})}}{dN}\right)\left[-\frac{\hbar^2}{2m}\nabla^2+V_H(\mathbf{r})+U_{\rm sub}(\mathbf{r})\right]\sqrt{\rho(\mathbf{r})} + \int d\mathbf{r}\,\rho(\mathbf{r})\frac{dV_H(\mathbf{r})}{dN}=\mu+N\left(\frac{d\mu}{dN}\right). \quad (2.18)$$

Upon taking into account the previous result (2.16), one obtains

$$\mu=2\int d\mathbf{r}\left(\frac{d\sqrt{\rho(\mathbf{r})}}{dN}\right)\left[-\frac{\hbar^2}{2m}\nabla^2+V_H(\mathbf{r})+U_{\rm sub}(\mathbf{r})\right]\sqrt{\rho(\mathbf{r})}. \quad (2.19)$$

This form indicates that chemical potential is given by a spatially weighted average over the left-hand side of the Hartree equation (1.4), where the normalized weight is twice the derivative of the square root of the one-body density with respect to the particle number. The result (2.19) is to be compared with that provided by Eq. (2.3)

$$\mu=\frac{1}{N}\int d\mathbf{r}\sqrt{\rho(\mathbf{r})}\left[-\frac{\hbar^2}{2m}\nabla^2+V_H(\mathbf{r})+U_{\rm sub}(\mathbf{r})\right]\sqrt{\rho(\mathbf{r})}. \quad (2.20)$$

Both expressions, (2.19) and (2.20), give the chemical potential at a fixed particle number. The difference between these forms lies in the fact that the latter one is exclusively written in terms of solutions of Eq. (1.4) determined at the selected N, whereas Eq. (2.19) also requires information about solutions at particle numbers lying in the vicinity of N. Hence, Eq. (2.19) may be used to control the overall self-consistency, likewise Eqs. (2.13) and (2.15). On the other hand, upon equating Eqs. (2.19) and (2.20), one gets the self-consistent ''closure'' relation

$$\int d\mathbf{r}\left(2\frac{d\sqrt{\rho(\mathbf{r})}}{dN}-\frac{\sqrt{\rho(\mathbf{r})}}{N}\right)\left[-\frac{\hbar^2}{2m}\nabla^2+V_H(\mathbf{r})+U_{\rm sub}(\mathbf{r})\right]\sqrt{\rho(\mathbf{r})}=0, \quad (2.21)$$

which may also be obtained by generalizing the identity

$$0=\int d\mathbf{r}\left(\frac{d\rho(\mathbf{r})}{dN}\right)-1=\int d\mathbf{r}\left(\frac{d\rho(\mathbf{r})}{dN}-\frac{\rho(\mathbf{r})}{N}\right)$$
$$=\int d\mathbf{r}\sqrt{\rho(\mathbf{r})}\left(2\frac{d\sqrt{\rho(\mathbf{r})}}{dN}-\frac{\sqrt{\rho(\mathbf{r})}}{N}\right). \quad (2.22)$$

III. THE CASE OF PLANAR SYMMETRY

The relations derived in the preceding section will be applied to examine the self-consistency of solutions obtained for planar films of liquid ^{4}He at zero absolute temperature. In the case of this symmetry, any one-body quantity becomes a one-dimensional function, $f(\mathbf{r})=f(z)$, depending only upon the z coordinate, which is the position of the atoms with respect to a fixed x-y plane determined by the substrate. Accordingly, the square root of the one-body density is determined by the one-dimensional version of the EL-equation (1.4)

$$\left[-\frac{\hbar^2}{2m}\frac{d^2}{dz^2}+V_H(z)+U_{\rm sub}(z)\right]\sqrt{\rho(z)}=\mu\sqrt{\rho(z)}. \quad (3.1)$$

For planar geometry, instead of solving this equation for a fixed value of N given by Eq. (1.3), one imposes the constraint on the particle number per unit area A denoted frequently as coverage

$$n_c=\frac{N}{A}=\int_0^\infty dz\,\rho(z). \quad (3.2)$$

Notice that here the liquid ^{4}He only occupies the $z>0$ half-space. In turn, the energy per particle becomes

$$e=\frac{E_{\rm gs}}{N}=\frac{1}{n_c}\left[\frac{\hbar^2}{2m}\int_0^\infty dz\left(\frac{d\sqrt{\rho(z)}}{dz}\right)^2+\int_0^\infty dz\,\rho(z)e_c(z)\right.$$
$$\left.+\int_0^\infty dz\,\rho(z)U_{\rm sub}(z)\right], \quad (3.3)$$

where the correlation energy per particle $e_c(z)$ depends on the approach adopted for $E_c(\mathbf{r},\mathbf{r}')$.

In practice, Eq. (3.1) is solved for fixed coverages and, subsequently, the energy per particle is evaluated by using the obtained solutions. This procedure yields the equation of state e as a function of n_c, which must satisfy the basic laws of thermodynamics. As known, at $T=0$ K the variation of the ground-state energy of a single-component system of N particles, which presents flat interfaces of area A, is given by[32–35]

$$dE_{\rm gs}=\sigma_A dA+\mu dN, \quad (3.4)$$

where σ_A is the surface tension (notice that in this case the pressure is zero). The formal thermodynamic definitions of σ_A and μ lead to the following expressions in terms of the energy per particle e,

$$\sigma_A=\left(\frac{\partial E_{\rm gs}}{\partial A}\right)_N=\left(\frac{\partial(E_{\rm gs}/N)}{\partial(A/N)}\right)_N=-n_c^2\frac{de}{dn_c}, \quad (3.5)$$

and

$$\mu=\left(\frac{\partial E_{\rm gs}}{\partial N}\right)_A=\left(\frac{\partial(E_{\rm gs}/A)}{\partial(N/A)}\right)_A=e+n_c\frac{de}{dn_c}. \quad (3.6)$$

These equations lead to the well-known relation that may be also derived starting from Eqs. (3.1) and (3.3)

$$\sigma_A=n_c(e-\mu)=\frac{E_{\rm gs}-\mu N}{A}=\frac{\Omega}{A}. \quad (3.7)$$

Here Ω is the thermodynamic grand potential at $T=0$ K. Within the framework of this formulation, a necessary condition for ensuring the stability of a system is to require a positive areal isothermal compressibility κ_s. As pointed out in Refs. 33 and 34, at $T=0$ K this condition may be expressed in the following way:

$$\frac{1}{\kappa_s}=A\left(\frac{\partial\sigma_A}{\partial A}\right)_N=\frac{A}{N}\left(\frac{\partial\sigma_A}{\partial(A/N)}\right)_N=-n_c\frac{d\sigma_A}{dn_c}>0. \quad (3.8)$$

It may be rewritten in terms of the incompressibility, which has the dimension of an energy and is related to the third-sound velocity c_3 (cf. the second cite of Ref. 4)

$$\frac{1}{n_c\kappa_s}=-\frac{d\sigma_A}{dn_c}=n_c\frac{d\mu}{dn_c}=mc_3^2>0. \quad (3.9)$$

At this point, one can make a connection to Eq. (2.16) derived in the preceding section. So, quantity c_3 may be calculated from the variation of the Hartree mean field

$$mc_3^2=n_c\frac{d\mu}{dn_c}=\int_0^\infty dz\,\rho(z)\frac{dV_H(z)}{dn_c}. \quad (3.10)$$

In order to study the energetics of planar films, it is useful to expand the energy per particle as a polynomial in powers of the inverse of coverage[33–35]

$$e=\frac{E_{\rm gs}}{N}=e_\infty+\sum_{k=1}^{\infty}\frac{a_k}{n_c^k}. \quad (3.11)$$

Here $e(n_c\to\infty)=e_\infty$ can be identified with the saturation equilibrium value for a three-dimensional uniform ^{4}He $e_B=-7.15$ K.[36]

The chemical potential derived by using Eqs. (3.11) and (3.6) becomes

$$\mu=e_\infty-\sum_{k=2}^{\infty}(k-1)\frac{a_k}{n_c^k}, \quad (3.12)$$

being independent of a_1. A further simplification can be achieved by taking into account that for thick enough slabs, only the van der Waals tail of the substrate-adsorbate potential,

$$U_{\rm sub}^{tail}(z)\simeq-\frac{C_{tail}}{z^3}, \quad (3.13)$$

is relevant for the growth of the system. As stated by Cheng and Cole,[37] in the large coverage regime, the chemical potential varies to first-order approximation as $1/n_c^3$

$$\mu \simeq e_\infty - \rho_0^3 \frac{\Gamma}{n_c^3}, \tag{3.14}$$

where $\rho_0 = 0.021\,836$ Å^{-3} is the equilibrium bulk density.[36] This result implies that the coefficient a_2 should be zero. According to the simplest version of the Frenkel-Halsay-Hill (FHH) model [see, e.g., Eq. (5) in Ref. 37, which has been derived by neglecting effects due to retardation of the van der Waals force], Γ is directly determined by the strength of the long-range tail of the interaction between ^{4}He and the substrate

$$\Gamma \simeq \Gamma_{\rm FHH} = \Delta C_{tail} \equiv C_{tail} - C_{tail}^{\rm He}, \tag{3.15}$$

with $C_{tail}^{\rm He} \simeq 120$ K Å^3 being the C coefficient of a hypothetical ^{4}He substrate. So the chemical potential of Eq. (3.12) may be rewritten as

$$\mu = e_\infty - 2\frac{\gamma_c}{n_c^3} - \sum_{k=4}^{\infty} (k-1)\frac{a_k}{n_c^k}, \tag{3.16}$$

where the main contribution due to the van der Waals tail was explicitly separated, and the coefficient a_3 was renamed

$$\gamma_c \equiv a_3. \tag{3.17}$$

The derivation of the surface tension by applying Eq. (3.5) to the expansion (3.11) leads to

$$\sigma_A = \sigma_\infty^{(\rm tot)} + 3\frac{\gamma_c}{n_c^2} + \sum_{k=4}^{\infty} k\frac{a_k}{n_c^{k-1}}, \tag{3.18}$$

where, as above, it was set $a_2 = 0$, and the coefficient a_1 was identified with the total surface tension in the limit of infinite width

$$a_1 = \lim_{n_c \to \infty} \sigma_A = \sigma_\infty^{(\rm tot)}. \tag{3.19}$$

The incompressibility may be expressed as

$$\frac{1}{n_c \kappa_s} = 6\frac{\gamma_c}{n_c^3} + \sum_{k=4}^{\infty} k(k-1)\frac{a_k}{n_c^k} > 0. \tag{3.20}$$

Perhaps it is worthwhile to stress that the incompressibility is independent of the quantities e_∞ and σ_∞; it depends on how the chemical potential and the surface tension reach these asymptotic values.

After taking into account the above-mentioned facts, the energy per particle may be written as

$$e = e_\infty + \frac{\sigma_\infty^{(\rm tot)}}{n_c} + \frac{\gamma_c}{n_c^3} + \sum_{k=4}^{\infty} \frac{a_k}{n_c^k}. \tag{3.21}$$

Notice that this expansion is a generalization of Eq. (25) reported in Ref. 34.

IV. RESULTS FOR ^{4}He ADSORBED ONTO A K SUBSTRATE

In this section, we describe the study of liquid ^{4}He films adsorbed on planar surfaces of K at zero absolute temperature. Both substrate-adsorbate potentials given by Eqs. (1.6) and (1.7) and displayed in Fig. 1 were examined. In order to facilitate a comparison, the well depths and the coefficients of the long-range tail of these potentials are listed in Table I together with the parameters of the ''3-9'' potential for a substrate of Na. The values quoted in Table I indicate that the depth D_{vdW} of the CCZ interaction lies in the middle of the D values for K and Na [see also Eq. (1.6)]. Furthermore, the long-range coefficient C_{vdW} is about 30% larger than C_3 for K and it is very close to C_3 for Na. In summary, the new adsorption potential for K is more similar to the ''3-9'' potential for Na than to that corresponding to K. The quantities of interest for the analysis of the films were determined by solving the Hartree-like equation (3.1). The results reported in the present work have been calculated by using two different approaches for the Hartree mean-field potential $V_H(z)$, namely, those given by the OP- and OT-NLDF formalisms. The corresponding expressions for $V_H(z)$ are provided elsewhere.[4,35,38] The overall consistency of the solutions has been checked by verifying that numerical results satisfy the variational relations derived in Sec. II.

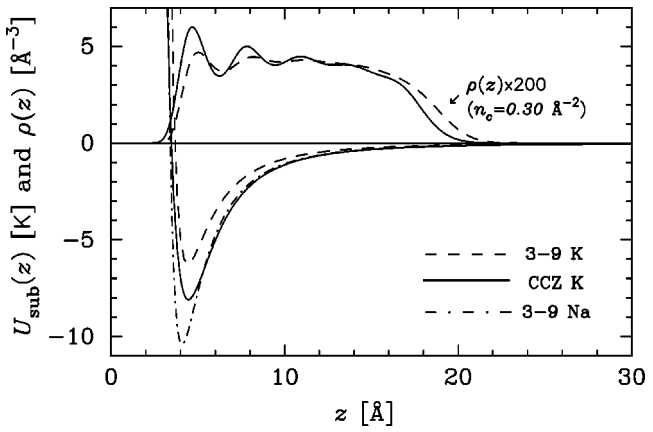

FIG. 1. Substrate-adsorbate potentials $U_{\rm sub}(z)$ as a function of the distance z from the surface. The dashed and solid curves are, respectively, the standard two parameter ''3-9'' potential and the most recent CCZ potential, both generated by a substrate of K. For comparison, the adsorption ''3-9'' potential for a substrate of Na is represented by a dot-dashed curve. Two extreme examples of the obtained density profiles $\rho(z)$ for $n_c = 0.30$ Å^{-2} are also plotted. The dashed curve shows the OP-NLDF results for the 3-9 potential, while the continuous curve corresponds to the OT-NLDF calculation with the CCZ potential.

The integrodifferential problem (3.1) has been solved for a large range of coverages up to $n_c = 0.40$ Å^{-2} in steps of $\delta n_c = 0.01$ Å^{-2}. This maximum coverage coincides with the

TABLE I. Comparison of the representative parameters of the ^{4}He-K adsorption potentials.

Substrate	$z_{\rm min}$ (Å) [a]		Depth (K)		C_{tail} (K Å^3)	
	3–9	CCZ	D [b]	D_{vdW} [c]	C_3 [b]	C_{vdW} [c]
K	4.42	4.48	6.26	8.11	812.0	1044.5
Na	4.09		10.4		1070.0	

[a]Quantity $z_{\rm min}$ is the coordinate at which the potentials attain their minimum values.

[b]These values correspond to the ''3-9'' potential.

[c]These values correspond to the CCZ potential of Ref. 29.

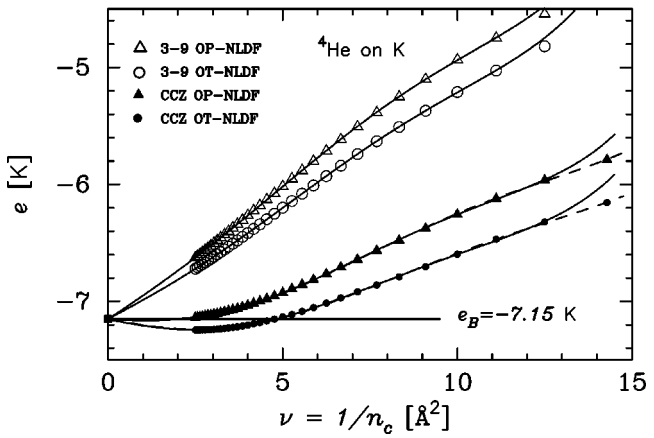

FIG. 2. Energy per particle $e=E_{gs}/N$ as a function of the inverse of coverage $\nu=1/n_c$. The symbols representing data calculated by using the different approaches outlined in the text are explicitly indicated. The full square is the bulk saturation value $e_B=-7.15$ K. The continuous curves show the fits to Eq. (4.6) including up to fifth-order terms. The dashed curves show the fit of all data to a sixth-order polynomial as explained in the text.

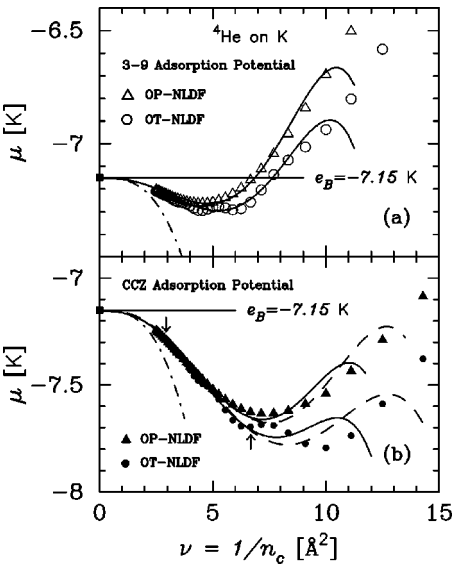

FIG. 3. Chemical potential as a function of the inverse of coverage $\nu=1/n_c$. The solid curves show μ evaluated with Eq. (3.12) by keeping up to fifth-order terms and using the parameters listed in Table II. The dash-dotted curve is the FHH approximation given by Eq. (4.2). (a) Results obtained for the ''3-9'' adsorption potential. (b) Same as (a) for the CCZ adsorption potential. In addition, the dashed curves show the results obtained with the sixth-order polynomial. The vertical arrows indicate the OT-NLDF values of μ for $n_c=0.15$ and 0.35 Å^{-2} used to calculate $\delta\mu$ for the example discussed in the text.

size of the biggest films calculated by Clements, Krotscheck, and Tymczak[39] in a recent analysis of the energetics of ^{4}He adsorbed on alkali-metal substrates of Cs, Na, and Li. In order to get $\rho(z)$ and μ, Eq. (3.1) has been discretized in a box of size $0<z\leqslant z_L=35$ Å, which insures that for the largest system the neglected $\sqrt{\rho(z)}$ were smaller than 10^{-5} Å$^{-3/2}$. Four solutions were determined for every coverage, i.e., one for each combination of the adsorption potentials $U_{sub}(z)$ and the NLDF formalisms mentioned above. Two sets of the one-body densities obtained for $n_c=0.30$ Å^{-2} are shown in Fig. 1. They correspond to the OP-NLDF results for the ''3-9'' potential and the OT-NLDF values for the CCZ potential, these data exhibit the largest difference among the four profiles evaluated for this coverage. Having determined $\rho(z)$ and the optimal Hartree mean-field potential $V_H(z)$, we evaluated the energy per particle e.

Figure 2 shows the results for e as a function of $\nu=1/n_c$. It becomes clear from this figure that the behavior of the solutions obtained for the ''3-9'' potential is significantly different from that exhibited by results corresponding to the CCZ potential. The values of the former series of e decrease monotonically toward the value e_B for increasing n_c (i.e., for $\nu=1/n_c\rightarrow 0$) showing a well-defined positive slope, while the results for the latter potential cross the value e_B at finite coverages and attain the asymptotic value from below. On the other hand, the energy values calculated with the OP-NLDF formalism lie systematically above the OT-NLDF results for both potentials.

The obtained values of μ are plotted as a function of $\nu=1/n_c$ in Fig. 3. From this drawing it becomes clear that, for all the investigated cases, very large films always satisfy the stability condition (3.9) written in terms of ν

$$n_c\frac{d\mu}{dn_c}=-\nu\frac{d\mu}{d\nu}>0, \tag{4.1}$$

suggesting a possible wetting of the potassium surface. The minimum coverage $n_c^{\min}$ that verifies this condition depends on the choice of $U_{sub}(z)$ and the adopted NLDF approach. Furthermore, Fig. 3 indicates that, for each substrate-adsorbate potential, the OP- and OT-NLDF results merge into one another at small ν (i.e., at large coverages $n_c\gtrsim 0.30$ Å^{-2}). This feature is due to the fact that for thick films, the behavior of μ is mainly determined by γ_c, which in turn depends on the van der Waals tail of the $U_{sub}(z)$. The size of this contribution can be estimated by using Eqs. (3.14) and (3.15)

$$\mu\simeq e_\infty-\rho_0^3\frac{C_{tail}-C_{tail}^{He}}{n_c^3}. \tag{4.2}$$

Figure 3 shows the results provided by this simple approximation when C_{tail} takes the values C_3 and C_{vdW} quoted in Table I. Notice that at medium coverages, the OT-NLDF data exhibit oscillations as a function of ν.

Let us now describe the verification of the relations required by Eqs. (2.13) and (2.15). We shall focus the attention on the consistency of solutions obtained for different coverages because wetting is related to the third-sound velocity, which in turn depends on the behavior of μ as a function of n_c. The variation of the chemical potential may be evaluated by using the simplified version of Eq. (2.13) written for planar symmetry, i.e.,

$$\delta\mu=\frac{\int_0^\infty dz\sqrt{\rho(z)}[\sqrt{\rho(z)}+\delta\sqrt{\rho(z)}]\delta V_H(z)}{\int_0^\infty dz\sqrt{\rho(z)}[\sqrt{\rho(z)}+\delta\sqrt{\rho(z)}]}. \tag{4.3}$$

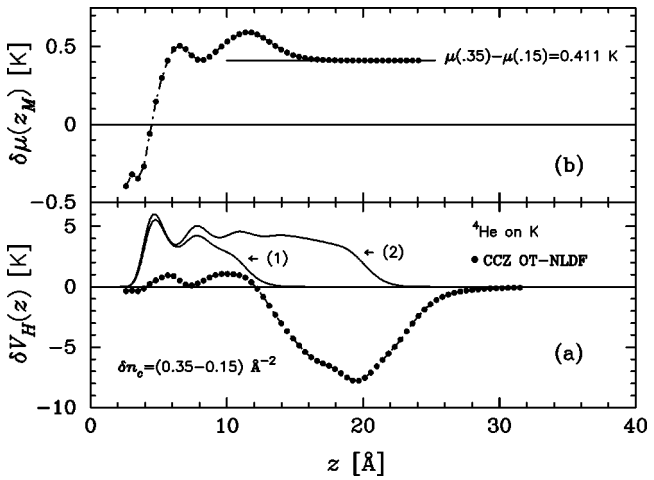

FIG. 4. (a) Variation of the Hartree mean-field potential as a function of distance z from the substrate. The full circles stand for data corresponding to the pair of coverages $n_{ci}=0.15$ Å^{-2} and $n_{cf}=0.35$ Å^{-2}, which were calculated within the OT-NLDF formalism for the CCZ potential. The continuous curves are the one-body densities $\rho(z)$ given in arbitrary units, the symbols (1) and (2) indicate, respectively, the profiles corresponding to the smaller and larger films. (b) Evolution of the change of chemical potentials evaluated with Eq. (4.4) for increasing z_M.

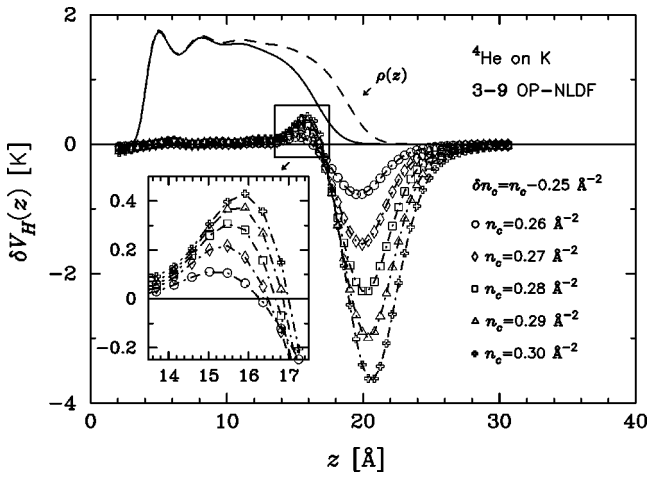

FIG. 5. The variation of the Hartree mean-field potential obtained within the OP-NLDF formalism for the ''3-9'' potential is shown as a function of the distance z from the surface. The plotted data correspond to pairs of coverages whose difference increases linearly according to $\delta n_c=n_c-0.25$ Å^{-2} with $n_c=0.26$, 0.27, 0.28, 0.29, and 0.30 Å^{-2}. The relevant positive contributions are magnified in the inset. The density profiles (displayed in arbitrary units) for $n_c=0.25$ Å^{-2} (continuous curve) and $n_c=0.30$ Å^{-2} (dashed curve) indicate clearly that values stemming from the surface region yield the crucial contributions.

It is worthwhile to emphasize the power of this equation for testing the consistency of solutions obtained for very different coverages. Let us illustrate this feature showing the behavior of the results provided by OT-NLDF calculations in the case of the CCZ potential for $n_{ci}=0.15$ Å^{-2} and $n_{cf}=0.35$ Å^{-2}. The difference between the values of μ yielded by Eq. (3.1) is $\delta\mu=0.411$ K [cf. Fig. 3(b)]. Figure 4(a) shows the variation of the Hartree mean-field potential for this pair of coverages as a function of z. It is instructive to follow the convergence of the ratio (4.3) introducing the limit of integration z_M

$$\delta\mu=\lim_{z_M\to\infty}\frac{\int_0^{z_M}dz\sqrt{\rho(z)}[\sqrt{\rho(z)}+\delta\sqrt{\rho(z)}]\delta V_H(z)}{\int_0^{z_M}dz\sqrt{\rho(z)}[\sqrt{\rho(z)}+\delta\sqrt{\rho(z)}]}. \tag{4.4}$$

Figure 4(b) indicates the evolution of Eq. (4.4) for increasing values of z_M. In the adopted notation, the horizontal line labeled by $\mu(.35)-\mu(.15)$ stands for the difference of values obtained at $n_{cf}=0.35$ Å^{-2} and $n_{ci}=0.15$ Å^{-2}. So, the convergence exhibited by the ratio of integrals is quite good, the limiting value is safely attained before the box size z_L is reached. Notice, that in spite of the large coverage difference, $\delta n_c=0.20$ Å^{-2}, the agreement between the value provided by Eq. (4.3) and that obtained from the two independent solutions of Eq. (3.1) is excellent.

We shall now report a careful analysis of the numerical results for the most controversial case corresponding to OP-NLDF calculations for the ''3-9'' adsorption potential. Looking at Fig. 3(a), one can guess that there is a minimum at about $n_c\simeq 0.22$ Å^{-2}. So, since we are primarily interested in checking the stability of the films, in the following lines we shall focus the attention on coverages bigger than this value. Figure 5 shows the results for pairs whose coverage difference increases linearly according to the relation $\delta n_c=n_c-0.25$ Å^{-2} with $n_c=0.26$, 0.27, 0.28, 0.29, and 0.30 Å^{-2}. This drawing indicates that for every δn_c, there are well-defined positive and negative contributions localized in the surface region. On the balance of these contributions depends whether a film is stable or not. The data shown in Fig. 5 can be used to check two different properties of the chemical potential. On the one hand, one can evaluate $\delta\mu$ corresponding to two different coverages by using Eq. (4.3). On the other hand, one can determine the slope $d\mu/dn_c$ by calculating the integral of Eq. (2.15).

Figure 6 shows results of the weighted averages over the values of $\delta V_H(z)$ calculated with Eq. (4.4) for the pairs of coverages given in the previous paragraph. The convergence of these ratios of integrals was examined as a function of z_M starting from the value $z_M=6.56$ Å corresponding to the completion of the first layer of liquid ^{4}He. This plot indicates that after exhibiting an initial positive value, the quantity $\delta\mu$ always strongly increases when the positive $\delta V_H(z)$ contributions displayed in the inset of Fig. 5 are included in the integrals, subsequently, $\delta\mu$ decreases dramatically when the negative contributions are included. However, in spite of the fact that the strength of the negative values of $\delta V_H(z)$ is larger than that of the positive ones, their total contribution is not enough to reverse the sign of $\delta\mu$ because the geometric average of the involved one-body densities $\rho(z)$ is small in that region of z. The solid horizontal lines displayed in Fig. 6 represent the differences between the chemical potentials yielded by the Hartree-like equation (3.1) for each one of the two involved coverages. From this figure, it becomes clear that data evaluated with Eq. (4.4) always converge to the differences $\delta\mu$ given by solutions of Eq. (3.1).

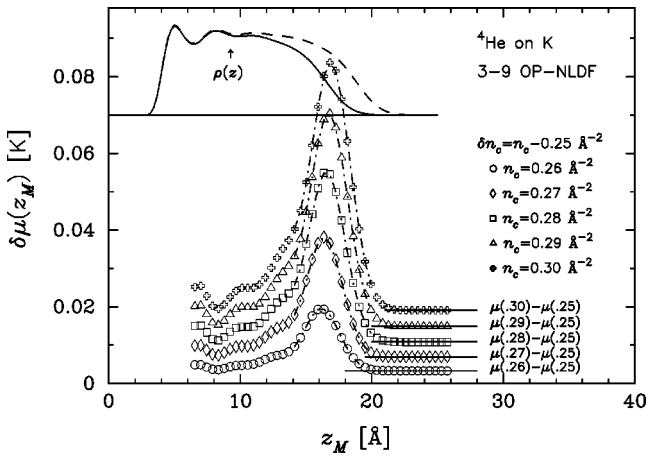

FIG. 6. Variation of the chemical potential given by the ratio of integrals (4.4) as a function of the limit of integration z_M for the same pairs of coverages considered in Fig. 5. The solid horizontal lines represent differences between the corresponding chemical potentials obtained directly from the solutions of Eq. (3.1) and plotted in Fig. 3(a). As in Fig. 5, the density profiles (displayed in arbitrary units) for $n_c=0.25$ Å^{-2} (continuous curve) and $n_c=0.30$ Å^{-2} (dashed curve) indicate clearly that values stemming from the surface region yield the crucial contributions.

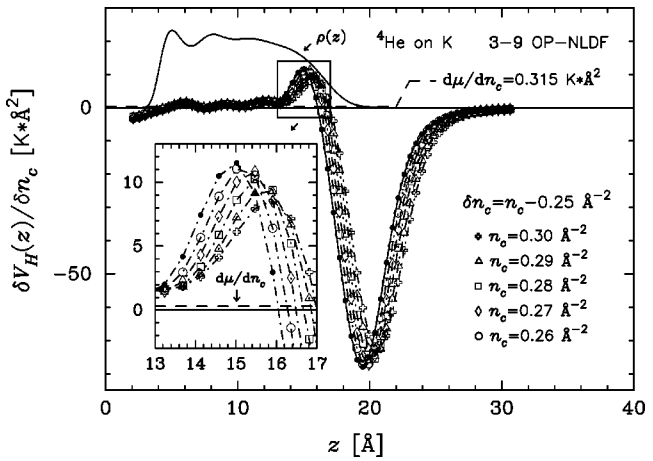

FIG. 7. Ratio of the variation of the Hartree mean-field potential to the variation of the coverage as a function of z for the same pairs of coverages considered in Fig. 5. Full circles joined by the solid curve indicate the limit of the ratio for $\delta n_c \to 0$. The continuous curve in the upper part stands for the density profile $\rho(z)$ of the film with coverage $n_c=0.25$ Å^{-2} plotted in arbitrary units. The derivative $d\mu/dn_c$ at $n_c=0.25$ Å^{-2} evaluated according to Eq. (4.5) by using the displayed values of $\lim_{\delta n_c \to 0}[\delta V_H(z)/\delta n_c]$ is indicated by the horizontal dashed line. The relevant positive contributions and $d\mu/dn_c$ are magnified in the inset.

We shall now examine the extent to which the numerical results satisfy the requisite imposed by (2.15). This requirement implies that at each n_c, the derivative $d\mu/dn_c$ must be equal to the weighted average over the values of $\lim_{\delta n_c \to 0}[\delta V_H(z)/\delta n_c]$, i.e.,

$$\frac{d\mu}{dn_c}=\frac{1}{n_c}\int_0^\infty dz\,\rho(z)\lim_{\delta n_c\to 0}\left(\frac{\delta V_H(z)}{\delta n_c}\right). \tag{4.5}$$

We illustrate this part of the study describing the behavior of ratios of the variation of the Hartree mean-field potential to the variation of the coverage corresponding to the same pairs of coverages considered in Fig. 5. Figure 7 shows $\delta V_H(z)/\delta n_c$ as a function of the position z. These ratios were used to determine the limit for $\delta n_c \to 0$ at each value of z. The obtained results are also plotted in Fig. 7 together with the density profile $\rho(z)$ for the film of $n_c=0.25$ Å^{-2} needed for the evaluation of the average. The computation of Eq. (4.5) yields $d\mu/dn_c=0.315$ K Å^2. Since this value agrees with the derivative calculated directly with the data plotted in Fig. 3(a), the necessary condition (4.5) is successfully verified.

In fact, we have calculated the local variations $\delta V_H(z)$ for all the pairs of considered coverages and verified the consistency of the solutions. In summary, this test has been satisfactorily applied to all the sets of data of μ displayed in Fig. 3 giving a strong support to the overall consistency of the solutions. Having checked this point, let us turn to the analysis of the data of e as a function of $1/n_c$.

In a first step, each set of $e(n_c)$ has been fitted to the polynomial

$$e=e_\infty+\frac{\sigma_\infty^{(\mathrm{tot})}}{n_c}+\frac{\gamma_c}{n_c^3}+\frac{a_4}{n_c^4}+\frac{a_5}{n_c^5}, \tag{4.6}$$

where all the coefficients of terms up to fifth-degree were left free, while all the coefficients a_k with $k>5$ were set at zero. In practice, this analysis has been extended to data covering the range $0\leqslant\nu\lesssim 11$ Å^2, where the value $e_B=-7.15$ K corresponding to bulk liquid at saturation[36] was included in the fits following the procedure discussed in Ref. 34. The extracted values of e_∞, $\sigma_\infty^{(\mathrm{tot})}$, γ_c, a_4, and a_5 are listed in Table II. As expected, all the results for e_∞ are consistent with e_B. For both adsorption potentials, the extracted values of γ_c are somewhat smaller than the corresponding FHH estimations indicating a retardation effect.[37] Figure 2 shows that fits of all the sets of energy data are quite good over the considered range of coverages.

The chemical potential evaluated by inputting the extracted parameters in Eq. (3.16) is displayed in Fig. 3. This plot indicates that such estimations reproduce satisfactorily well the values of μ obtained from the solutions of Eq. (3.1) up to $\nu\simeq 9$ Å^2 (i.e., small coverages of about $n_c\simeq 0.11$ Å^{-2}), except for the CCZ OT-NLDF case where the agreement is good only up to $\nu\simeq 7$ Å^2 ($n_c\simeq 0.15$ Å^{-2}). Notice that for very thick films (small values of ν) the fitting curves merge into the lowest-order approximation given by Eq. (4.2). Table II also contains the values $n_c^{\min}$ indicating the coverages at which the initial negative slopes $d\mu(n_c)/dn_c$ are reversed. Since $n_c^{\min}\geqslant 0.10$ Å^{-2}, the stability of thin films with $n_c\simeq 0.043$ Å^{-2} is ruled out in agreement with the finding of Boninsegni and Cole.[21]

For the sake of completeness, we have performed a second fit of the energy data corresponding to the CCZ potential including here all the values plotted in Fig. 2. In this case, the term a_6/n_c^6 was added to Eq. (4.6) and in the fitting procedure two coefficients were taken fixed, namely, $e_\infty=e_B$ and $\gamma_c=\gamma_{\mathrm{CCZ}}^0$. The extracted values are also quoted in Table II. This extension improves, at small coverages, the

TABLE II. Coefficients of the expansion for the energy per particle e for ^{4}He adsorbed on a potassium substrate.

System	Data source		e_∞ (K)	$\sigma_\infty^{(\mathrm{tot})}$ (K/Å^4)	$\gamma_c\times10^3$ (K/Å^6)	$a_4\times10^3$ (K/Å^8)	$a_5\times10^3$ (K/Å^{10})	$a_6\times10^6$ (K/Å^{12})	$n_c^{\min}$ (Å^{-2})
Bulk ^{4}He	Experiment								
	e_B		−7.15 [a]						
^{4}He-K	Theory								
	Adsorption Potential	Formalism							
	"3–9" [b]	FHH [c] (γ_{3-9}^0)			3.60				
		OP-NLDF	−7.153	0.1997	2.78	−0.422	0.0167		0.22
		OT-NLDF	−7.151	0.1597	2.91	−0.421	0.0164		0.17
	CCZ [d]	FHH [c] (γ_{CCZ}^0)			4.81				
		OP-NLDF	−7.154	−0.0129	4.46	−0.512	0.0169		0.14
			−7.15 [e]	−0.0132	4.46 [e]	−0.545	0.0232	−0.302	
		OT-NLDF	−7.155	−0.0561	4.48	−0.501	0.0164		0.10
			−7.15 [e]	−0.0562	4.48 [e]	−0.539	0.0238	−0.349	

[a]Bulk energy per particle quoted in Table II of Ref. 36 and used for fixing the parameters of both examined NLDF formalisms.
[b]Standard two-parameter adsorption potential.
[c]Coefficient γ_c estimated by using the FHH approach as explained in text.
[d]Adsorption potential proposed in Ref. 29.
[e]These values were kept fixed.

fits for e and the predictions for μ as can be seen in Figs. 2 and 3(b), respectively. However, the oscillations of μ obtained within the OT-NLDF approach (caused by the layered structure of the films) cannot be described with the polynomial expression of the type (3.21). This feature is also present, although attenuated, in the case of the "3-9" potential.

Let us now center the attention on the wetting. It was found that, in all the analyzed cases, the chemical potential determined for films of large coverages satisfy the necessary condition for stability (3.9). However, according to Dzyaloshinskii, Lifshitz, and Pitaevskii[40] (see discussion of Fig. 12 therein), for insuring a permanent complete wetting of the investigated substrate, one must also examine the behavior of the grand potential per unit area σ_A given by Eq. (3.18). The "true" stable state of the film corresponds to that for which σ_A is a minimum. In practice, when searching for wetting, one should compare the asymptotic value of the surface grand potential

$$\sigma_A(n_c\to\infty)=\frac{\Omega(n_c\to\infty)}{A}=\sigma_\infty^{(\mathrm{tot})}, \tag{4.7}$$

with $\sigma_A(n_c=0)=0$ (see Fig. 8 in the second cite of Ref. 4). The values of $\sigma_\infty^{(\mathrm{tot})}$ quoted in Table II indicate that the wetting is guaranteed in the case of the CCZ potential, while the standard "3-9" interaction leads to metastable states.

V. CONCLUDING REMARKS

In the present work, we studied the stability of liquid ^{4}He films adsorbed to planar surfaces of K. Two different proposals for the interaction between ^{4}He atoms and the potassium surface have been examined. These are the standard "3-9" substrate-adsorbate potential and a more elaborated one developed by Chizmeshya, Cole, and Zaremba,[29] both versions are given in Sec. I. The calculations have been performed within the framework of two different NLDF formalisms, namely, those known as Orsay-Paris[6] and Orsay-Trento[27] functionals. A special effort was devoted in order to analyze the consistency of solutions corresponding to different coverages. For this purpose, variational relations have been derived for the chemical potential, which is a crucial quantity of this problem.

Let us now briefly summarize our investigation concerning the variational properties of the Hartree-like equation (1.4). We proved that if the ground-state energy of a many-body Bose system is written as a functional of the particle distribution $\rho(\mathbf{r})$ according to Eq. (1.1) and consequently $\sqrt{\rho(\mathbf{r})}$ is determined by Eq. (1.4), then the solutions for finite systems must present variations satisfying the relation (2.13). We would like to stress the remarkable simplicity of the latter equation, which expresses that the variation of the chemical potential μ for finite changes of the particle number N is given by a sort of weighted average over the local variations of the Hartree mean-field potential $V_H(\mathbf{r})$. Besides the intrinsic beauty of this compact form, it should be emphasized that Eq. (2.13) may be used as a tool to control the overall self-consistency of evaluated solutions. In particular, the results for the chemical potential μ, which is the least stable quantity, can be tested. Furthermore, the limit for infinitesimal variations (2.15) yields that the derivative of μ with respect to N may be written as a weighted average over the local derivatives $dV_H(\mathbf{r})/dN$.

In light of the obtained results, we concluded that all the numerical solutions determined in this study satisfy with high accuracy the derived variational properties written for the planar geometry. In the case of this symmetry, the derivative $d\mu/dn_c$ has physical importance because it is related to the stability of a Bose many-body system [cf., Eq. (3.9)].

An important result of this investigation is the finding

that, for every combination of the examined $U_{\rm sub}(z)$ potentials and utilized NLDF approaches, when n_c grows continuously from a certain minimum coverage to ∞ then μ approaches the asymptotic value $e_\infty = e_B = -7.15$ K from below (see Fig. 3). This behavior is in agreement with the description of wetting given in the first cite of Ref. 4. Even for the weaker interaction, i.e., the ''3-9'' potential, the present calculations for thick enough films yielded positive values of the square of the third-sound velocity, $mc_3^2 = n_c d\mu/dn_c$. However, the additional condition outlined in Ref. 40 which in practice requires a negative $\sigma_\infty^{(\rm tot)}$ is not satisfied by the results obtained with the ''3-9'' potential. Therefore, the standard ''3-9'' adsorption potential used for the potassium substrate in Refs. 4 and 27 may only lead to metastable films. On the other hand, the stronger CCZ potential yields $\sigma_\infty^{(\rm tot)} < 0$ for both analyzed NLDF approaches. In summary, on the basis of results provided by the more elaborated adsorption potential we can state that the liquid ^{4}He wets the surface of K at $T = 0$ K. This feature is in agreement with the experimental evidence.[9,18]

In addition, in all the examined cases, our results support the finding of Boninsegni and Cole[21] that thin quasi-two-dimensional films with $n_c \simeq 0.043$ Å^{-2} are unstable.

ACKNOWLEDGMENTS

This work was supported in part by the Ministry of Culture and Education of Argentina through Grants PIP-CONICET No. 4486/96 and SIP No. EX-01/TX55.

*Also at the Carrera del Investigador Científico of the Consejo Nacional de Investigaciones Científicas y Técnicas, Av. Rivadavia 1917, RA-1033 Buenos Aires, Argentina.

[1] *Proceedings of the International Symposium on Quantum Fluids and Solids* [J. Low Temp. Phys. **101**, (1/4) (1995)].
[2] *Proceedings of the International Symposium on Quantum Fluids and Solids* [J. Low Temp. Phys. **110**, (1/2) (1998)].
[3] *Proceedings of the International Symposium on Quantum Fluids and Solids* [J. Low Temp. Phys. **113**, (3/6) (1998)].
[4] E. Cheng, M. W. Cole, W. F. Saam, and J. Treiner, Phys. Rev. Lett. **67**, 1007 (1991); Phys. Rev. B **46**, 13 967 (1992); **47**, 14 661(E) (1993).
[5] E. Cheng, M. W. Cole, J. Dupont-Roc, W. F. Saam, and J. Treiner, Rev. Mod. Phys. **65**, 557 (1993).
[6] J. Dupont-Roc, M. Himbert, N. Pavloff, and J. Treiner, J. Low Temp. Phys. **81**, 31 (1990).
[7] E. Zaremba and W. Kohn, Phys. Rev. B **15**, 1769 (1977).
[8] R. B. Hallock, J. Low Temp. Phys. **101**, 31 (1995).
[9] P. J. Nacher and J. Dupont-Roc, Phys. Rev. Lett. **67**, 2966 (1991); P. J. Nacher, B. Demolder, and J. Dupont-Roc, Physica B **194-196**, 975 (1994).
[10] K. S. Ketola, S. Wang, and R. B. Hallock, Phys. Rev. Lett. **68**, 201 (1992).
[11] S. K. Mukherjee, D. P. Druist, and M. H. W. Chan, J. Low Temp. Phys. **87**, 113 (1992).
[12] P. Taborek and J. E. Rutledge, Phys. Rev. Lett. **68**, 2184 (1992); J. E. Rutledge and P. Taborek, *ibid.* **69**, 937 (1992); P. Taborek and J. E. Rutledge, *ibid.* **71**, 263 (1993); Physica B **197**, 283 (1994).
[13] P. Stefanyi, J. Klier, and A. F. G. Wyatt, Phys. Rev. Lett. **73**, 692 (1994).
[14] N. Bigelow, P. J. Nacher, and J. Dupont-Roc, J. Low Temp. Phys. **89**, 135 (1992); B. Demolder, N. Bigelow, P. J. Nacher, and J. Dupont-Roc, *ibid.* **98**, 91 (1995).
[15] G. Mistura, H. C. Lee, and M. H. W. Chan, Physica B **194-196**, 661 (1994).
[16] A. F. G. Wyatt, J. Klier, and P. Stefanyi, Phys. Rev. Lett. **74**, 1151 (1995).
[17] T. A. Moreau and R. B. Hallock, J. Low Temp. Phys. **110**, 659 (1998).
[18] J. A. Phillips, P. Taborek, and J. E. Rutledge, J. Low Temp. Phys. **113**, 829 (1998).
[19] J. A. Phillips, D. Ross, P. Taborek, and J. E. Rutledge, Phys. Rev. B **58**, 3361 (1998).
[20] G. Mistura, H. C. Lee, and M. H. W. Chan, J. Low Temp. Phys. **89**, 633 (1992).
[21] M. Boninsegni and M. W. Cole, J. Low Temp. Phys. **113**, 393 (1998).
[22] M. Boninsegni, M. W. Cole, and F. Toigo, Phys. Rev. Lett. **83**, 2002 (1999).
[23] J. Klier, P. Stefanyi, and A. F. G. Wyatt, Phys. Rev. Lett. **75**, 3709 (1995); J. Klier and A. F. G. Wyatt, Czech. J. Phys. **46**, 439 (1996); J. Low Temp. Phys. **110**, 919 (1998).
[24] E. Rolley and C. Guthmann, J. Low Temp. Phys. **108**, 1 (1997).
[25] D. Ross, J. E. Rutledge, and P. Taborek, Science **278**, 664 (1997); D. Ross, P. Taborek, and J. E. Rutledge, J. Low Temp. Phys. **111**, 1 (1998).
[26] F. Ancilotto, A. M. Sartori, and F. Toigo, Phys. Rev. B **58**, 5085 (1998).
[27] F. Dalfovo, A. Lastri, L. Pricaupenko, S. Stringari, and J. Treiner, Phys. Rev. B **52**, 1193 (1995).
[28] A. Lastri, F. Dalfovo, L. Pitaevskii, and S. Stringari, J. Low Temp. Phys. **96**, 227 (1995).
[29] A. Chizmeshya, M. W. Cole, and E. Zaremba, J. Low Temp. Phys. **110**, 677 (1998).
[30] M. Boninsegni and M. W. Cole, J. Low Temp. Phys. **110**, 685 (1998).
[31] R. A. Aziz, V. P. S. Nain, J. S. Carley, W. L. Taylor, and G. T. McConville, J. Chem. Phys. **70**, 4330 (1979); R. A. Aziz, M. J. Slaman, A. Koide, A. R. Allnat, and W. J. Meath, Mol. Phys. **77**, 321 (1992).
[32] J. S. Rowlinson and B. Widom, *Molecular Theory of Capillarity* (Clarendon, Oxford, 1982).
[33] L. Szybisz, Phys. Rev. B **58**, 109 (1998).
[34] L. Szybisz, J. Low Temp. Phys. **116**, 215 (1999).
[35] L. Szybisz, Eur. Phys. J. B **14**, 733 (2000).
[36] S. Stringari and J. Treiner, Phys. Rev. B **36**, 8369 (1987).
[37] E. Cheng and M. W. Cole, Phys. Rev. B **38**, 987 (1989), and references therein.
[38] L. Szybisz, Phys. Rev. B **56**, 11 845 (1997).
[39] B. E. Clements, E. Krotscheck, and C. J. Tymczak, J. Low Temp. Phys. **107**, 387 (1997).
[40] I. E. Dzyaloshinskii, E. M. Lifshitz, and L. P. Pitaevskii, Adv. Phys. **10**, 165 (1961).